Materials Advances

ROYAL SOCIETY OF CHEMISTRY

PAPER

View Article Online
View Journal | View Issue

Cite this: *Mater. Adv.*, 2022, 3, 599

2,9-Dibenzo[*b*,*def*]chrysene as a building block for organic electronics†

Félix Gagnon,[a] Vicky Tremblay,[a] Armand Soldera,[b] Michael U. Ocheje,[c] Simon Rondeau-Gagné,[c] Mario Leclerc[a] and Jean-François Morin*[a]

Received 2nd September 2021,
Accepted 8th November 2021

DOI: 10.1039/d1ma00799h

rsc.li/materials-advances

In this article, a new series of conjugated polymers based on a low-cost, easily accessible vat dye called Vat orange 1 or 2,9-dibromo-dibenzo[*b*,*def*]chrysene-7,14-dione have been prepared. This compound was made electron-donating by reducing and alkylating the ketone groups into alkoxy groups, allowing the introduction of solubilizing, branched alkyl chains at the 7 and 14 positions. Polymerization reactions using Suzuki–Miyaura coupling with 6,6′-isoindigo, 3,6-di-2-thienyl-pyrrolo[3,4-*c*]pyrrole-1,4-dione (DPP) and 4,7-dithieno-2,1,3-benzothiadiazole (TBT) yielded three donor–acceptor polymers with band-gap values ranging from 1.61 to 1.86 eV. Field-effect transistors (OFETs) and organic solar cells (OSCs) were fabricated and hole mobility values of up to 3.62 × 10^{-4} cm^2 V^{-1} s^{-1} and a maximum power conversion efficiency of 1.2% were measured, respectively.

Introduction

Dyes possessing a carbon-rich, extended π-conjugated core are promising building blocks for the preparation of semiconductors in organic electronics due to their relatively low cost, stability and ease of functionalization.[1–3] In fact, many of them possess synthetic handles such as halogens and ketones that allow easy chemical functionalization and modifications of their electronic properties. Recently, vat orange 3 (4,10-dibromoanthanthrone) has been used as the starting material for several π-conjugated molecules and polymers for multiple applications, including field-effect transistors,[4–7] light-emitting diodes,[8,9] aggregation-induced emission (AIE),[10] solar cells[11–17] and singlet fission.[18,19] This dye showed good versatility as it can be functionalized at the 4, 6, 10 and 12 positions to yield materials with a wide range of properties.[20–27] However, the major drawback of this dye is the presence of two hydrogen atoms at the *peri* position relative to the two bromine atoms (4 and 10 positions) that cause significant steric hindrance with the neighbouring conjugated units.[28] This structural flaw in regard to the effective conjugation length along with its neutral electronic nature (neither a donor nor an acceptor) makes the synthesis of low bandgap materials based on vat orange 3 very challenging. To overcome this problem, strategies such as the introduction of conjugated spacers such as alkene or alkyne moieties and rigidification through the formation of a carbon bridge to eliminate the *peri* proton have been explored.[17,28,29] Unfortunately, none of them succeed in significantly decreasing the bandgap of anthanthrone-based molecules and polymers.

Thus, other similar vat dyes have to be explored in order to prepare low bandgap materials that would be suitable for organic electronics applications. Among the commercially available dihalogenated vat dyes, vat orange 1 is particularly appealing since it possesses two bromine atoms at the 2 and 9 positions where virtually no steric hindrance could lead to a high dihedral angle. Moreover, this dye also has two ketones (like vat orange 3), allowing a wide variety of chemical modifications.

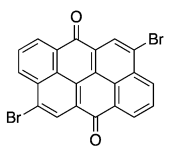

Vat orange 3

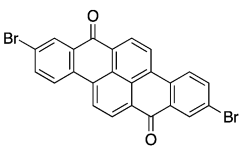

Vat orange 1
(*This work*)

Herein, we report the synthesis, characterization and device performances of conjugated polymers based on 2,9-dibenzo[*b*,*def*]chrysene (vat orange 1). In order to ensure the solubility of the polymers, the dye was alkylated at the 7 and 14 positions

[a] *Département de chimie and Centre de Recherche sur les Matériaux Avancés (CERMA), 1045 Ave de la Médecine, Université Laval, Québec, QC, G1V 0A6, Canada. E-mail: jean-francois.morin@chm.ulaval.ca*
[b] *Laboratory of Physical Chemistry of Matters, Department of chemistry, Faculty of science, 2500 Boulevard de l'Université, Université de Sherbrooke, Sherbrooke, QC, J1K 2R1, Canada*
[c] *Department of Chemistry and Biochemistry, 401 Sunset Avenue, University of Windsor, Windsor, ON, N9B 3P4, Canada*

† Electronic supplementary information (ESI) available. See DOI: 10.1039/d1ma00799h

to give two electron-donor alkoxy groups. This unit was then polymerized with three different electron-accepting units, namely isoindigo (**P1**), diketopyrrolopyrrole (**P2**) and bisthiophenylbenzothiadiazole (**P3**). The polymers were characterized and tested as semiconductors in field-effect transistors and bulk heterojunction solar cells.

Results and discussion

The synthesis of **P1–P3** is described in Scheme 1. In order to ensure the solubility of **P1–P3**, 2,9-dibromo-dibenzo[*b*,*def*]chrysene-7,14-dione (vat orange 1) was first alkylated using a branched alkyl chain using an adapted protocol developed for vat orange 3 to obtain compound **1**.[20] Then, a two-fold Miyaura borylation reaction under standard conditions obtained compound **2** in 53% yield. **P1–P3** were prepared by Suzuki coupling using the same procedure by coupling compound **2** with isoindigo, DPP and TTBT, respectively. After the synthesis, the polymers were purified by precipitation in methanol, followed by washing with methanol, hexanes and chloroform using a Soxhlet apparatus to remove the oligomers and the catalyst residues. The reaction yield for each polymer was calculated using the soluble fraction only. The molecular weight values (M_n and M_w) of **P1–P3** were measured by size-exclusion chromatography using polystyrene standards and 1,2,4-trichlorochlorobenzene as the eluent at 110 °C (Table 1).

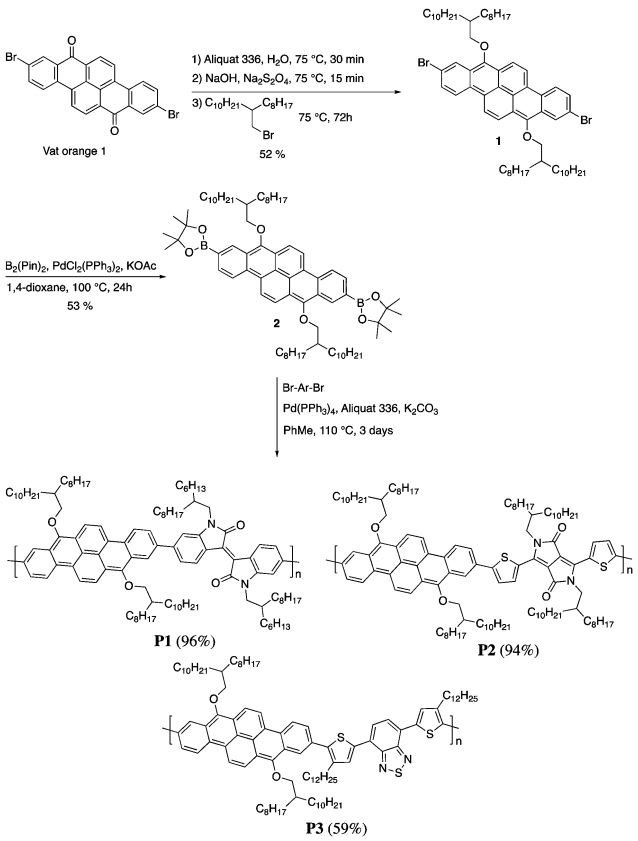

Scheme 1 Synthesis of **P1–P3**.

Table 1 Molecular weights and dispersity indexes of **P1–P3**

Polymer	$\overline{M_n}$ (kg mol^{-1})^a	$\overline{M_w}$ (kg mol^{-1})^a	$Đ^a$ ($\overline{M_w}/\overline{M_n}$)	X_n
P1	33	53	1.6	21
P2	46	119	2.6	26
P3	42	95	2.2	28

$\overline{M_n}$: the number average molecular weight. $\overline{M_w}$: the weight average molecular weight. $Đ$: dispersity index. ^{a} Molecular weight values and $Đ$ values of **P1**, **P2** and **P3** were measured by SEC at 110 °C using 1,2,4-trichlorobenzene as the eluent and polystyrene as the standard.

Number average molecular weight (M_n) values ranging from 33 to 46 kg mol^{-1} were obtained, corresponding to the degree of polymerization (X_n) values between 21 and 28, providing good film-forming properties.

Thermal properties were measured using differential scanning calorimetry (DSC) and thermogravimetric analysis (TGA) and the results are shown in Fig. S9–S12 (ESI†). In all cases, the measured glass transition temperature (T_g) values were between 100 and 120 °C and no melting transition was observed, meaning that **P1–P3** are amorphous. These observations agree with the nature of the long, branched alkyl chain attached to the 2,9-dibenzo[*b*,*def*]chrysene unit.[30] TGA analysis was performed under a nitrogen atmosphere at a heating rate of 10 °C per minute. Decomposition temperature (T_d) values between 280 and 290 °C (taken a 5% weight) were measured for all three polymers, indicating that the most sensitive part of the polymers is likely the 2,9-dibenzo[*b*,*def*]chrysene unit. These T_d values are similar to those measured for the conjugated polymers based on anthanthrene (vat orange 3).[29] Although these values are lower than those of most conjugated polymers, they are high enough to ensure good thermal stability of the polymers for device fabrication and operation.

The optical properties in both the solution and solid states of **P1–P3** are shown in Fig. 1 and are summarized in Table 2. All the polymers showed a broad absorption band in the UV–visible region with λ_{max} values ranging from 478 to 700 nm in solution. For **P1**, the band in the high energy region centered at 478 nm can be attributed to the π–π* transition while the broad band centered at 572 nm is attributed to the

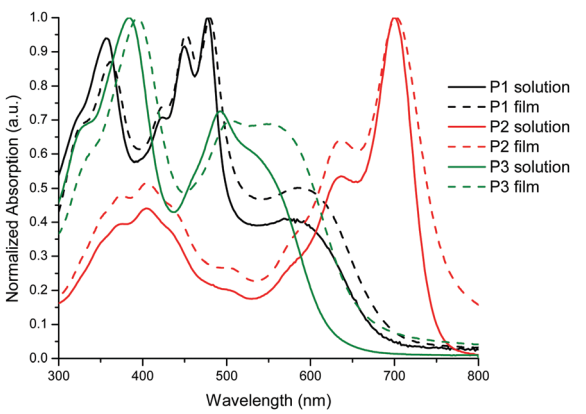

Fig. 1 Normalized UV–vis absorption spectra of polymers **P1–P3** in a solution of $CHCl_3$ and as a thin film.

Table 2 Photophysical and electrochemical properties of the polymers

Polymer	λ_{max}^{sol} nm [a]	λ_{max}^{film} nm [b]	E_g^{opt} (eV) [c]	E_{HOMO} (eV) [d]	E_{LUMO} (eV) [d]	E_g^{elec} (eV)
P1	478	480	1.77	−5.36	−3.49	1.86
P2	700	702	1.61	−5.31	−3.73	1.58
P3	492	506	1.86	−5.35	−3.40	1.95

[a] Solution in chloroform. [b] Spin cast film from chloroform solution. [c] The optical bandgap values were estimated from the edge of the absorption spectra of thin films ($E_g^{opt} = 1240/\lambda_{onset}$). [d] HOMO and LUMO energy levels were calculated using the formula $E_{HOMO} = -(4.71 + E_{onset}^{ox})$ eV and $E_{LUMO} = -(4.71 + E_{onset}^{re})$ eV, in which E_{onset}^{ox} and E_{onset}^{re} are the oxidation onset potential (the CV thin film) and the reduction onset potential (the CV thin film), respectively, *versus* SCE.

presence of a charge transfer complex between the dibenzo[*b*,*def*]chrysene and isoindigo units.[31] Interestingly, the solid state spectrum exhibits only a slight bathochromic shift compared to that in solution, indicating that the polymer backbone conformation is very similar in both states. The same behavior was also observed for **P2** and **P3**.

As reported previously for BTD-based conjugated polymers,[32,33] **P3** exhibits two sets of absorption bands centered at 384 and 492 nm. Interestingly, the shoulder at 540 nm in the solution UV–visible spectrum, associated to the presence of an intramolecular donor–acceptor complex, increased in intensity in the solid state while becoming broader towards the low energy region of the spectrum. This can be attributed to a planarization of the polymer backbone in the solid state, making the charge transfer complex between the 2,9-dibenzo[*b*,*def*]chrysene and BTD units more efficient. All the polymers exhibit a bandgap value below 1.9 eV (see Table 2), the lowest value being obtained for **P2** (1.61 eV). These values correlate well with those measured using electrochemistry in thin films. As expected, the HOMO energy values for **P1–P3** are very similar since they are governed by the donor unit that is the same for all three polymers (2,9-dibenzo[*b*,*def*]chrysene unit). For the LUMO, **P2** exhibits the lowest energy value at −3.73 eV, which is suitable to undergo charge transfer upon excitation with most of the electron-acceptor molecules used in the fabrication of solar cells.

Theoretical calculations

DFT calculations were performed on the dimers of the three polymers to assess their conformation, the energy levels, and the frontier orbitals distribution using the Gaussian 09 software.[34] Research on the conformation of the minimum energy was first carried out. For this, each part, the vat orange derivative with the bromine atoms substituted by ethyl chains, and the three groups, were first optimized. To find the minimum of energy for the final molecule, the bond between the two parts was rotated by 10 degrees, and the potential energy was computed for each dihedral angle. The density functional theory (DFT) approach was considered using 6-31G** as the basis set and B3LYP as the functional. The dihedral angle corresponds to four consecutive carbon atoms.

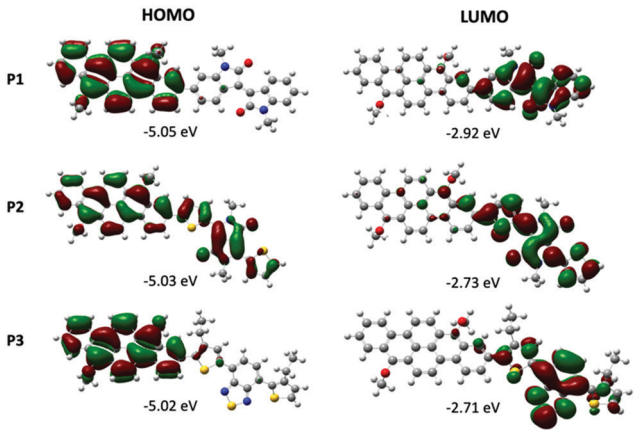

Fig. 2 Kohn–Sham molecular orbitals of dimers of **P1**, **P2** and **P3** based on calculation at the B3LYP/6-31G(d,p) level.

Of the three polymers, **P2** is the one presenting the lowest dihedral angle (θ = 30.3°) between the vat orange 1 and the comonomer (see Table S3 and Fig. S23 in the ESI† section). For **P1** and **P3**, the presence of phenyl and an alkyl chain at the 3 position of thiophene induces a wider dihedral angle (θ = 40.6° and 44.9°, respectively). The low θ value in **P2** can partially explain the lower bandgap value (E_g = 1.61 eV).

For all three polymers, the HOMO orbital is mainly localized on the 2,9-dibenzo[*b*,*def*]chrysene unit, except for **P2** in which the HOMO is delocalized over the entire dimer (Fig. 2). As expected, the LUMO orbital is located almost exclusively on the electron-withdrawing unit. The bandgap values calculated for the dimers of **P1**, **P2** and **P3** are 2.13, 2.30 and 2.31, respectively.

Field-effect transistors (OFETs)

To investigate the influence of the acceptor moiety on the field-effect mobility and charge transport, bottom-gate, top-contact organic field-effect transistors (OFETs) were fabricated.

Table 3 Average and maximum hole mobility ($\mu_{h,av}$ and $\mu_{h,max}$), threshold voltages (V_{th}), I_{on}/I_{off}, and ratios for OFETs fabricated from **P1–P3**. Measurements performed after thermal annealing at 150 °C for 30 minutes under a N_2 atmosphere, average measured from 5 different devices

Polymer	W L^{-1}	μ_h^{max} ($\times 10^{-4}$ cm^2 V^{-1} s^{-1})	μ_h^{avg} ($\times 10^{-4}$ cm^2 V^{-1} s^{-1})	$I_{ON/OFF}$	V_{th} (V)
P1	10	0.635	0.245 ± 0.257	10^2	−14.46
P2	10	3.62	2.99 ± 0.624	10^3	−11.11
P3	10	3.36	3.22 ± 0.0912	10^3	−9.53

The device parameters and the extrapolated figures of merit are shown in Table 3 and fabrication procedures and device characteristics are detailed in the ESI.† The devices prepared from **P1**, containing the isoindigo acceptor, exhibited a relatively low mobility (2.45×10^{-5} cm^2 V^{-1} s^{-1}) and a low $I_{ON/OFF}$ current ratio. The devices prepared from **P1** also possess the highest threshold voltage of −14.46 V. In contrast, **P2**, which contains the diketopyrrolopyrrole acceptor, exhibits a higher charge mobility and better charge transport (an average mobility of 2.99×10^{-4} cm^2 V^{-1} s^{-1}), and overall device characteristics. For **P3**, which contains benzothiadiazole, an average field-effect mobility of 3.22×10^{-4} cm^2 V^{-1} s^{-1}, an $I_{ON/OFF}$ of 10^3 and a threshold voltage of −9.53 V were measured. Despite the important differences in charge transport between the three semiconducting polymers, all devices showed typical transfer and output characteristics as depicted in Fig. S22 (ESI†).

Organic solar cells (OSCs)

P1–P3 were tested in organic solar cells (OSCs) as p-type materials and the results are summarized in Table 4. The devices were prepared in an inverted geometry using [6,6]-phenyl-C61-butyric acid methyl ester ($PC_{61}BM$) as the electron acceptor in the heterojunction blend. The geometry studied was ITO/ZnO/Polymer:$PC_{61}BM$/MoO_3/Ag. Different ratios of diphenyl ether (DPE) as an additive in the active layer were tested (0, 1 and 2% V/V) to achieve the highest power conversion efficiency (PCE) for each polymer.[35] **P1** obtained a PCE of 0.25% without any additive. Under these conditions, **P1** achieved the highest open-circuit voltage (V_{OC} = 0.86 V) of the series, which is in accordance with the HOMO level of the polymer compared to **P2** and **P3**. **P2** obtained a quite a bit better PCE of 0.66% using 2% V/V DPE. This polymer gave a short-circuit current density (J_{SC}) four times better than that of **P1** (2.30 mA cm^{-2} *vs.* 0.577 mA cm^{-2}), but loses its gain because of a poor fill factor (FF) of 0.387 (**P1**:0.51). **P3** achieved the highest J_{SC}, FF and PCE of the series with 2.8 mA cm^{-2}, 0.53 and 1.2%, respectively, using 1% V/V DPE.

In the case where no additive was used, **P2** performances were very low, worse than **P1**, probably because the LUMO of **P2** (−3.73 eV) is similar to $PC_{61}BM$'s.[36] For **P1** and **P3**, their differences in performance may be due to the dihedral angle between the donor and acceptor units.

Table 4 Organic solar cell results[a] for the devices made from **P1–P3**

Polymer	Additive ratio[b] (% V/V)	J_{sc} (mA cm^{-2})	V_{oc} (V)	FF	PCE (%)
P1[c]	—	0.577	0.86	0.51	0.25
P2	—	0.9	0.8	0.33	0.2
	2	2.30	0.74	0.387	0.66
P3	—	2.50	0.84	0.50	1.05
	1	2.8	0.810	0.53	1.2

[a] Maximum values reached are presented here, and the average values are presented in the ESI. [b] Diphenyl ether as the additive. [c] No increase in performance observed using the additive with this polymer.

Conclusions

In conclusion, three donor–acceptor polymers based on vat orange 1 were synthesized using Suzuki coupling. All three polymers are highly soluble in common organic solvents and exhibit excellent film-forming properties. As shown by DFT calculations, the dialkoxy form of vat orange 1 is an electron-donor on which most of the HOMO frontier orbital is localized when coupled to the electron-deficient π-conjugated units. All polymers possess a bandgap value of under 1.9 eV, making them suitable for applications in solar cells. Moreover, they all exhibit hole-transporting properties in field-effect transistors. Thus, vat orange 1 proved to be an efficient, low-cost building block for the preparation of the conjugated polymers for organic electronics.

Conflicts of interest

There are no conflicts to declare.

Acknowledgements

The authors thank the National Science and Engineering Council of Canada (NSERC) for financial support. Félix Gagnon thanks the NSERC and FRQNT for a Master scholarship. We are also grateful for professional support from CQMF and CERMA. The computational resources were provided by Calcul Québec and Compute Canada, through financial support of the Canadian Foundation Innovation (CFI). Simon Rondeau-Gagné acknowledges financial support from the NSERC through a Discovery Grant (RGPIN-2017-06611) and the Canadian Foundation for Innovation (CFI). Michael U. Ocheje thanks the NSERC for a PhD scholarship.

Notes and references

1 D. Thetford and A. P. Chorlton, *Dyes Pigm.*, 2004, **61**, 49–62.
2 C. Aumaitre and J.-F. Morin, *Chem. Rec.*, 2019, **19**, 1142–1154.
3 J. F. Morin, *J. Mater. Chem. C*, 2017, 12298–12307.
4 Q. Liu, Y. Wang, L. Arunagiri, M. Khatib, S. Manzhos, K. Feron, S. E. Bottle, H. Haick, H. Yan, T. Michinobu and P. Sonar, *Mater. Adv.*, 2020, **1**, 3428–3438.
5 J. B. Giguère, N. S. Sariciftci and J. F. Morin, *J. Mater. Chem. C*, 2015, **3**, 601–606.
6 M. Irimia-Vladu, P. A. Troshin, M. Reisinger, G. Schwabegger, M. Ullah, R. Schwoediauer, A. Mumyatov, M. Bodea, J. W. Fergus, V. F. Razumov, H. Sitter, S. Bauer and N. S. Sariciftci, *Org. Electron.*, 2010, **11**, 1974–1990.
7 E. D. Glowacki, L. Leonat, G. Voss, M. Bodea, Z. Bozkurt, M. Irimia-Vladu, S. Bauer and N. S. Sariciftci, *Org. Semicond. Sensors Bioelectron. IV*, 2011, **8118**, 81180M.
8 B. K. Shah, D. C. Neckers, J. Shi, E. W. Forsythe and D. Morton, *Chem. Mater.*, 2006, **18**, 603–608.
9 B. K. Shah, D. C. Neckers, J. Shi, E. W. Forsythe and D. Morton, *J. Phys. Chem. A*, 2005, **109**, 7677–7681.

10 M. Desroches and J. F. Morin, *Org. Lett.*, 2018, **20**, 2797–2801.
11 H. D. Pham, T. T. Do, J. Kim, C. Charbonneau, S. Manzhos, K. Feron, W. C. Tsoi, J. R. Durrant, S. M. Jain and P. Sonar, *Adv. Energy Mater.*, 2018, **8**, 1–13.
12 H. D. Pham, K. Hayasake, J. Kim, T. T. Do, H. Matsui, S. Manzhos, K. Feron, S. Tokito, T. Watson, W. C. Tsoi, N. Motta, J. R. Durrant, S. M. Jain and P. Sonar, *J. Mater. Chem. C*, 2018, **6**, 3699–3708.
13 Y. Geng, C. Yi, M. P. Bircher, S. Decurtins, M. Cascella, M. Grätzel and S. X. Liu, *RSC Adv.*, 2015, **5**, 98643–98652.
14 J. Hong, Y. J. Kim, Y. H. Kim and C. E. Park, *Macromol. Chem. Phys.*, 2016, **217**, 2116–2124.
15 L. Zhang, B. Walker, F. Liu, N. S. Colella, S. C. B. Mannsfeld, J. J. Watkins, T.-Q. Nguyen and A. L. Briseno, *J. Mater. Chem.*, 2012, **22**, 4266–4268.
16 Y. J. Kim, J. S. Lee, J. Hong, Y. Kim, S. B. Lee, S. K. Kwon, Y. H. Kim and C. E. Park, *J. Polym. Sci., Part A: Polym. Chem.*, 2016, **54**, 2559–2570.
17 S. V. John, V. Cimrová, C. Ulbricht, V. Pokorná, A. Ružička, J. B. Giguère, A. Lafleur-Lambert, J. F. Morin, E. Iwuoha and D. A. M. Egbe, *Macromolecules*, 2017, **50**, 8357–8371.
18 Y. Jue Bae, M. D. Krzyaniak, M. B. Majewski, M. Desroches, J. F. Morin, Y. L. Wu and M. R. Wasielewski, *ChemPlusChem*, 2019, **84**, 1432–1438.
19 S. K. Sugunan, C. Greenwald, M. F. Paige and R. P. Steer, *J. Phys. Chem. A*, 2013, **117**, 5419–5427.
20 J. B. Giguère, Q. Verolet and J. F. Morin, *Chem. – Eur. J.*, 2013, **19**, 372–381.
21 J. B. Giguère, J. Boismenu-Lavoie and J. F. Morin, *J. Org. Chem.*, 2014, **79**, 2404–2418.
22 J.-B. Giguère and J.-F. Morin, *J. Org. Chem.*, 2015, 80.
23 U. Koldemir, J. S. Tinkham, R. Johnson, B. Lim, H. A. Yemam, K. J. Gagnon, S. Parkin and A. Sellinger, *J. Mater. Chem. C*, 2017, **5**, 8723–8733.
24 Y. Du, H. B. Lovell, F. Lirette, J. F. Morin and K. N. Plunkett, *J. Org. Chem.*, 2021, **86**, 1456–1461.
25 P. W. Münich, M. Pfäffli, M. Volland, S. X. Liu, R. Häner and D. M. Guldi, *Nanoscale*, 2020, **12**, 956–966.
26 C. Aumaitre, D. Fong, A. Adronov and J. F. Morin, *Polym. Chem.*, 2019, **10**, 6440–6446.
27 J.-B. Giguère, Q. Verolet and J.-F. Morin, *Chem. – Eur. J.*, 2013, **19**, 372–381.
28 F. Lirette, C. Aumaitre, C. É. Fecteau, P. A. Johnson and J. F. Morin, *ACS Omega*, 2019, **4**, 14742–14749.
29 A. Lafleur-Lambert, J. B. Giguère and J. F. Morin, *Polym. Chem.*, 2015, **6**, 4859–4863.
30 R. Xie, A. R. Weisen, Y. Lee, M. A. Aplan, A. M. Fenton, A. E. Masucci, F. Kempe, M. Sommer, C. W. Pester, R. H. Colby and E. D. Gomez, *Nat. Commun.*, 2020, **11**, 893.
31 X. Xu, L. Li, B. Liu and Y. Zou, *Appl. Phys. Lett.*, 2011, **98**, 063303.
32 J. D. Harris, M. Stihl, H. W. Schmidt and K. R. Carter, *J. Polym. Sci., Part A: Polym. Chem.*, 2019, **57**, 60–69.
33 K. W. Song, M. H. Choi, H. J. Song, S. W. Heo, J. Y. Lee and D. K. Moon, *Sol. Energy Mater. Sol. Cells*, 2014, **120**, 303–309.
34 M. J. Frisch, G. W. Trucks, H. B. Schlegel, G. E. Scuseria, M. A. Robb, J. R. Cheeseman, G. Scalmani, V. Barone, G. A. Petersson, H. Nakatsuji, X. Li, M. Caricato, A. Marenich, J. Bloino, B. G. Janesko, R. Gomperts, B. Mennucci, H. P. Hratchian, J. V. Ortiz, A. F. Izmaylov, J. L. Sonnenberg, D. Williams-Young, F. Ding, F. Lipparini, F. Egidi, J. Goings, B. Peng, A. Petrone, T. Henderson, D. Ranasinghe, V. G. Zakrzewski, J. Gao, N. Rega, G. Zheng, W. Liang, M. Hada, M. Ehara, K. Toyota, R. Fukuda, J. Hasegawa, M. Ishida, T. Nakajima, Y. Honda, O. Kitao, H. Nakai, T. Vreven, K. Throssell, J. A. Montgomery Jr., J. E. Peralta, F. Ogliaro, M. Bearpark, J. J. Heyd, E. Brothers, K. N. Kudin, V. N. Staroverov, T. Keith, R. Kobayashi, J. Normand, K. Raghavachari, A. Rendell, J. C. Burant, S. S. Iyengar, J. Tomasi, M. Cossi, J. M. Millam, M. Klene, C. Adamo, R. Cammi, J. W. Ochterski, R. L. Martin, K. Morokuma, O. Farkas, J. B. Foresman and D. J. Fox, *Gaussian 09, Revision A.02*, Gaussian, Inc., Wallingford CT, 2016.
35 E. F. Manley, J. Strzalka, T. J. Fauvell, T. J. Marks and L. X. Chen, *Adv. Energy Mater.*, 2018, **8**, 1–20.
36 X. Gong, T. Yu, Y. Cao and A. J. Heeger, *Sci. China: Chem.*, 2012, **55**, 743–748.